

EFFECTS OF SOIL NON-LINEARITY ON THE SEISMIC RESPONSE OF RIGID NON-SLIDING RETAINING WALLS

Yiannis TSOMPANAKIS¹, Prodromos N. PSARROPOULOS²,
Varvara ZANIA³, and Stefanos TSIMPOURAKIS⁴

ABSTRACT

The present paper aims to examine how and to what extent the potential soil non-linearity may affect both the dynamic distress of a rigid non-sliding retaining wall and the seismic response of the retained soil layer. For this purpose a parametric study, based on two-dimensional dynamic finite-element analyses, is conducted. Soil non-linearity is taken into account with sufficient realism via the commonly used *equivalent-linear* procedure. To examine more thoroughly the influence of material non-linearity the developed numerical model is studied under various idealized seismic excitations and several intensity levels of imposed ground acceleration. The results of the study justify the perception that non-linear soil behavior has a considerable impact, not only on the dynamic earth pressures developed on the wall, but on the amplification of the acceleration developed on the backfill as well. Therefore, it becomes evident that seismic norms and geotechnical design practice should take this impact into serious consideration.

Keywords: *retaining walls, dynamic interaction, soil non-linear behavior*

INTRODUCTION

Retaining walls have many applications in geotechnical engineering practice. Harbor quay-walls, bridge abutments, or deep excavations are some of the cases where a rigid gravity retaining wall or a flexible cantilever retaining wall is constructed. Despite their structural simplicity, the seismic response of walls (retaining even a single soil layer) is a rather complicated problem. What makes that response so complicated is the dynamic interaction between the wall and the retained soil, especially when material and/or geometry non-linearities are present [Kramer, 1996; PIANC, 2001; Wu and Finn, 1999; Green and Ebeling, 2002].

The seismic response of various types of walls that support a single soil layer has been examined by a number of researchers in the past, either experimentally, analytically, or numerically [Veletsos and Younan, 1997; Iai, 1998; Psarropoulos et al., 2005]. Depending on the assumed material behavior of the retained soil and the possible mode of the wall displacement, there exist two main categories of analytical methods used in the design of retaining walls against earthquakes: (a) the *pseudo-static methods* incorporating the limiting-equilibrium concept (Mononobe–Okabe type solutions) which

¹ Assistant Professor, Division of Mechanics, Department of Applied Sciences, Technical University of Crete, Greece, Email: jt@mechanics.tuc.gr

² Lecturer, Department of Infrastructure Engineering, Hellenic Air-Force Academy, Athens, Greece, Email: prod@central.ntua.gr

³ Doctoral Candidate, Division of Mechanics, Department of Applied Sciences, Technical University of Crete, Greece, Email: barbarazania@yahoo.gr

⁴ Postgraduate Student, School of Civil Engineering, National Technical University of Athens, Greece, Email: steftsim@tee.gr

assume yielding walls and rigid – perfectly plastic behavior of the retained soil [Okabe, 1926; Mononobe and Matsuo, 1929; Seed and Whitman, 1970], and (b) the *elasticity-based solutions* that regard the retained soil as a visco-elastic continuum [Scott, 1973; Wood, 1975; Veletsos and Younan, 1997].

According to an efficient simplification of the Mononobe-Okabe method, developed by Seed and Whitman (1970), the (maximum) normalized dynamic active earth force acting on the wall is:

$$\overline{\Delta P}_{AE} = \frac{\Delta P_{AE}}{A\rho H^2} \approx 0.4 \quad (1)$$

where A is the peak base acceleration, ρ is the soil mass density, and H is the wall height. At the same time, the elastic solutions developed in the early '70s by Scott (1973) and Wood (1975) suggest that in the case of low-frequency (quasi-static) base motions, which refers to many practical problems, the normalized dynamic active earth force developed on a rigid, non-sliding wall is:

$$\overline{\Delta P}_{AE} \approx 1 \quad (2)$$

that is almost 2.5 times more than the Seed and Whitman proposal. We have to mention that, as it will be shown later on, this discrepancy may be even more intense when the fundamental frequency of the base excitation approaches that of the retained soil layer under one-dimensional (1-D) conditions, i.e.

$$f_o = \frac{V_s}{4H} = \frac{\sqrt{G_{\max}/\rho}}{4H} \quad (3)$$

where V_s is the shear-wave velocity of the soil, and G_{\max} is its small-strain shear modulus.

However, the two aforementioned modes of wall–soil system behavior are rather extreme and do not always reflect reality since in many cases the assumptions of each method are not present. The limiting-equilibrium solutions imply the capability of the system to develop relatively large displacements (*geometric non-linearity*) together with the formation of plastic zones (*material non-linearity*). On the other hand, the elasticity-based solutions include only the potential geometric non-linearity by taking into account the wall flexibility and/or the wall foundation compliance [Veletsos & Younan, 1997]. In some real cases, like bridge abutments, braced excavations, and basement walls, the presence of kinematic constraints on the wall motion, is incompatible with the limiting-equilibrium concept while, on the other hand, the available elasticity-based solutions overlook the potential non-linear behavior of the retained soil, thus leading to over-conservative design.

The objective of the present study is to examine more thoroughly the influence of material non-linearity on the dynamic distress of a wall retaining a single soil layer. For this purpose two-dimensional numerical simulations are performed, utilizing the finite-element method, in order to investigate some of the most important aspects of this complex phenomenon of dynamic non-linear wall-soil interaction. In order to “isolate” the effects of material non-linearity on the system response, the wall is considered rigid and non-sliding (Figure 1). Apart from the dynamic earth pressures developed on the wall, emphasis is put on the soil amplification of the base acceleration. Note that seismic norms (like the Eurocode 8 (EC8, 2004) or the Greek Seismic Code (EAK, 2000)), being based on limit-equilibrium methods, ignore both the true dynamic earth pressures and the potential soil amplification. A parametric study has been performed in order to examine how the level of applied acceleration may affect the earth pressures induced on the retaining wall. Material non-linearity is taken into account in a simplistic, yet efficient, way, through the use of an iterative equivalent-linear procedure in which strain-compatible shear modulus G and critical damping ratio ξ are used to describe the soil behavior within each iteration.

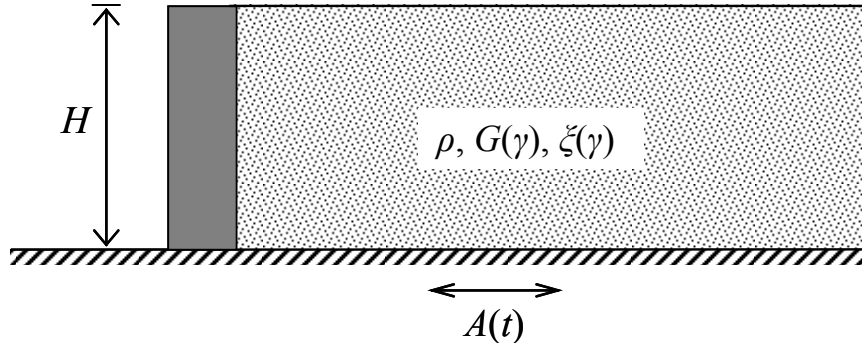


Figure 1. The retaining system examined in the present study: a rigid, non-sliding wall retaining a single soil layer with strain-dependent material behavior.

Dynamic response of any system depends on the seismic excitation characteristics (both in the time and in the frequency domain). However, in the present numerical study, the excitations were limited to harmonic and simple pulses in order to examine more thoroughly the complex phenomena of non-linear dynamic wall-soil interaction. Results provide a clear indication of the direct dynamic interaction between a retaining wall and the retained soil, whilst potential soil non-linearity seems to increase the degree of complexity, being either beneficial or detrimental for the wall distress, depending on the circumstances. That fact justifies the necessity for a more elaborate consideration of these interrelated phenomena on the seismic design of retaining walls.

NUMERICAL MODELING

In order to examine the non-linear dynamic wall-soil interaction, 2-D numerical simulations of the retaining system depicted in Figure 1 were conducted. The simulations were performed utilizing the QUAD4M finite-element code [Hudson et al. 1993], which performs dynamic non-linear analyses incorporating the well-known iterative equivalent-linear procedure. Each iteration includes: (a) a linear direct-integration dynamic analysis of the model, (b) the calculation of the maximum *effective shear strain* γ_{eff} for each element (calculated as a percentage of the maximum strain), and (c) the calculation of the strain-compatible shear modulus $G(\gamma_{eff})$ and critical damping ratio $\zeta(\gamma_{eff})$ to be used in the next iteration, by means of $G/G_{max} - \gamma$ and $\zeta - \gamma$ curves. The procedure terminates when convergence of G and ζ arises. The $G/G_{max} - \gamma$ and $\zeta - \gamma$ curves used are characteristic of sandy soil material [Seed & Idriss 1970; Idriss, 1990].

In general, the soil material properties (G, ρ) and the wall height alone do not affect the dynamic pressures on the wall, as the wall flexibility is examined in relation to soil stiffness and the earth pressures are normalized with ρ and H [Veletsos & Younan, 1997; Psarropoulos et al., 2005]. Therefore, all the analyses in the current investigation were performed considering an 8m-high wall. The retained soil layer is characterized by a relatively low small-strain shear-wave velocity V_s equal to 100m/s and a mass density of 1.8 Mg/m³. The discretization of the retained soil was performed by four-node plane-strain quadrilateral elements. The model was long enough so as to reproduce adequately the free-field conditions at the right-hand side of the model (see Figure 1). The rigid wall was simulated by an extremely stiff column with linear elastic behavior. The simplifying assumption that no de-bonding or relative slip is allowed to occur at the wall-soil interface was used.

The base of both the wall and the soil stratum were considered to be excited by a horizontal motion, assuming an equivalent force-excited system. The model was subjected to harmonic excitations of two different frequencies, the first matching the fundamental frequency of the soil layer f_o , and the second with frequency six times lower ($f = f_o/6$), to approximate a quasi-static excitation. Various levels of input acceleration were used, aiming at the development of different degrees of material non-linearity.

LINEAR HARMONIC RESPONSE

The dynamic linear response of a single soil layer under 1-D conditions has been studied by many researchers and analytical solutions for harmonic excitation can be found in the literature [Roesset, 1977; Kramer, 1996]. In the case of the harmonic excitation the response is controlled by the ratio f/f_o , where f is the dominant period of the excitation, and f_o the fundamental period of the soil layer. In our case the fundamental frequency of the soil layer $f_o \approx 3.1\text{Hz}$ (or equivalently, the fundamental period of the soil layer $T_o = 0.32\text{s}$). The duration of the sinusoidal pulse was such that steady state conditions were reached. In that case the maximum amplification factor (AF) for linear response is given by:

$$AF \cong \frac{2}{\pi\zeta} \frac{1}{2n+1} \quad (4)$$

where ζ is the critical damping ratio and n the eigen-mode number. For first mode ($n = 0$) and $\zeta = 5\%$, $AF \approx 12.5$

The presence of a retaining wall essentially imposes a vertical boundary condition, leading thus to a 2-D dynamic response. In this study the response of the soil layer under 1-D conditions is compared with the corresponding 2-D due to the existence of the wall (see Figure 1). The distribution of the amplification factor (AF) on the surface of the backfill in the case of the harmonic excitation at resonance ($f = f_o$) is plotted in Figure 2. It is evident that, for the rigid non-sliding wall, the motion in the vicinity of the wall is practically induced by the wall itself, and therefore no amplification is observed ($AF \approx 1$). The amplification factor converges to its maximum value ($AF \approx 12.5$) at a distance longer than $6H$ from the wall, since at that distance 1-D conditions are present (*free-field motion*).

Figure 3 presents the height-wise distribution of the normalized induced dynamic earth pressures for the two harmonic excitations examined. It can be observed that when the fundamental frequency of the input motion f approaches that of the retained soil layer f_o , the normalized dynamic earth force $\overline{\Delta P}_{AE}$ is almost three times greater for the case of resonance as opposed to a value almost equal to 1 for the case of quasi-static excitation (see also Equation (2)).

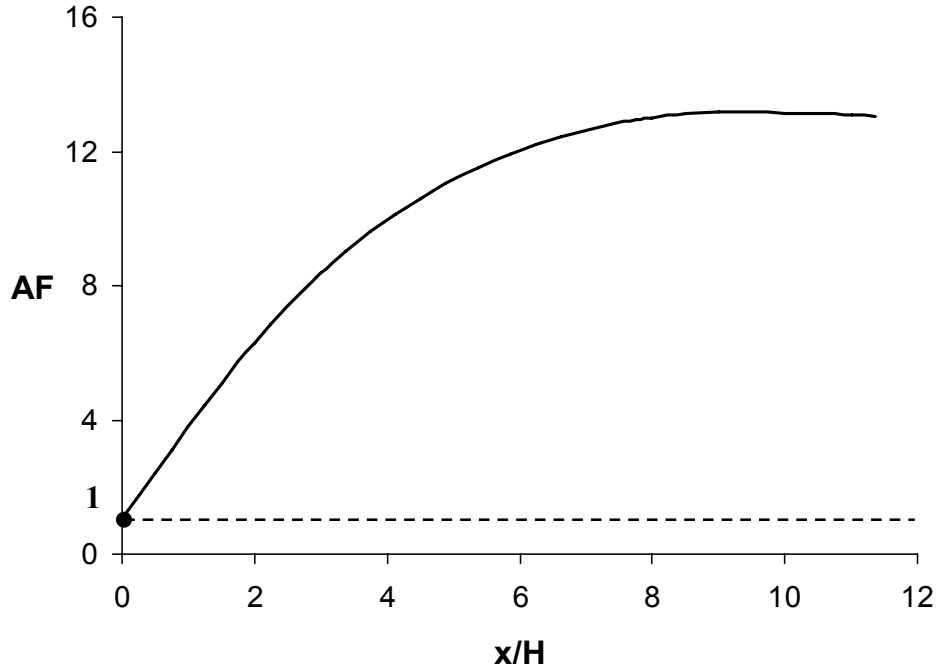


Figure 2. Distribution of the soil amplification factor (AF) along the surface of the backfill in the case of the harmonic excitation at resonance ($f = f_o$). Note that AF just behind the rigid wall examined is equal to unity.

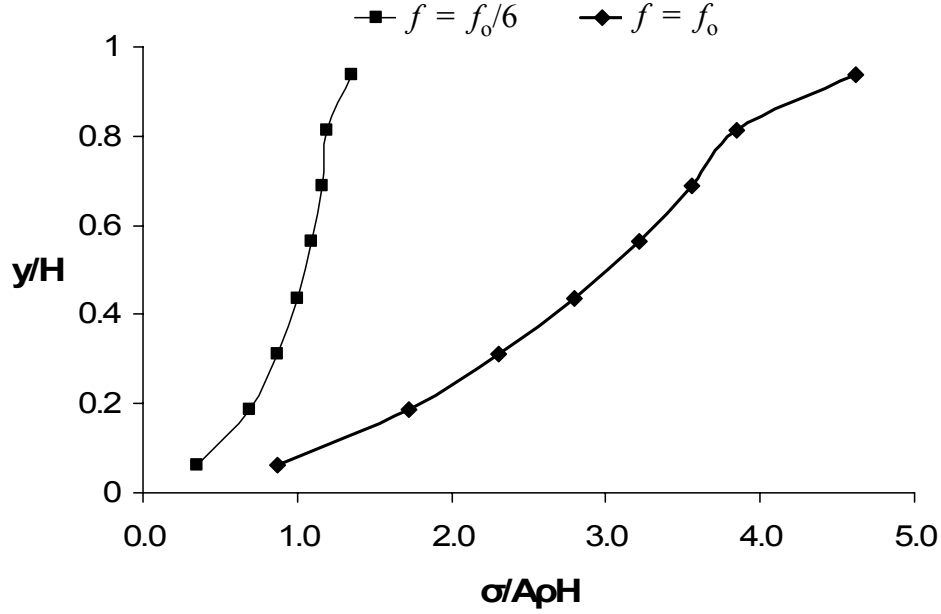


Figure 3. Height-wise distribution of the normalized induced dynamic earth pressures for the two harmonic excitations examined.

NON-LINEAR HARMONIC RESPONSE

The aforementioned results referring to the case of linear soil behavior are valid for very low levels of base input acceleration, when the induced strains remain small ($\gamma < 0.005\%$). However when the maximum acceleration acting on the soil mass reaches more realistic values, the induced strains are significantly greater, and thus the effects of material non-linearity (expressed by the $G/G_{\max} - \gamma$ and $\xi - \gamma$ curves) become more evident. The wall-soil system behavior depends heavily not only on the level of applied acceleration, but also on the f/f_0 ratio, a fact that arises from the following results.

The distribution of the amplification factor on the surface of the backfill in the case of the harmonic excitation at resonance ($f = f_0$) is plotted in Figure 4, for five levels of peak base acceleration: 0.001g (corresponding to linear soil behavior), 0.12g, 0.24g, 0.36g, and 0.50g, covering a broad range of induced dynamic strains. As expected, the increasing degree of material non-linearity makes the system “softer”, decreases its fundamental frequency, and leads to detuning, a phenomenon observed on the substantially reduced values of AF .

In addition, Figure 5 shows the height-wise distribution of the normalized induced dynamic earth pressures for the five levels of peak base acceleration examined in the case of the harmonic excitation at resonance. As the level of applied acceleration increases, the dynamic earth pressures are decreased. In fact, the normalized dynamic earth force on the wall reduces to values ranging from 0.6 to 0.9 (corresponding to $A = 0.50g$ and $A = 0.12g$, respectively) as opposed to the previously calculated value of 3 for the linear soil behavior case. It is evident that in the case of excitations with a fundamental frequency approaching that of the retained soil layer, the material non-linearity seems to act only in a beneficial way.

The case of quasi-static excitation is of greater interest. In Figure 6 the height-wise distribution of the normalized induced dynamic earth pressures is plotted in the case of the low-frequency harmonic excitation ($f = f_0/6$) for the five levels of peak base acceleration examined. Figure 7 stems from the results shown in Figures 5 and 6, as it shows $\overline{\Delta P_{AE}}$ as a function of peak base acceleration A . In the same Figure the values of Equations (1) and (2) are plotted as a reference.

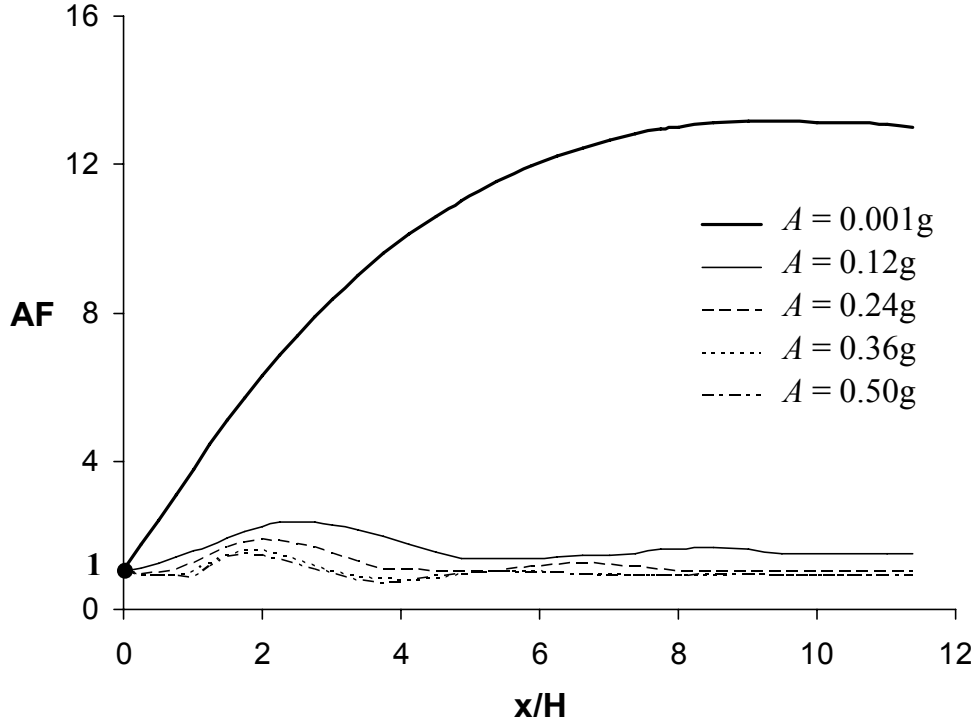


Figure 4. Distribution of the soil amplification factor (AF) along the surface of the backfill in the case of the harmonic excitation at resonance ($f = f_o$). All five cases of peak base acceleration are shown.

One could notice that:

- (a) as it was expected, in the linear case (i.e. $A = 0.001g$) the normalized dynamic earth force approaches the value of 1, and
- (b) for medium levels of peak base acceleration (i.e. $A = 0.24g$), the normalized dynamic earth pressures are maximized being higher than the values both of linear (i.e. $A = 0.001g$) or highly non-linear response (i.e. $A = 0.50g$).

This seeming discrepancy is attributed to the fact that at certain increased levels of induced strain, the aforementioned “softening” of the wall-soil system shifts its fundamental frequency closer to resonance with the applied input excitation, and thus to an increased distress. For even higher levels of induced strain, the resonance is avoided. Therefore, in the case of low-frequency harmonic excitation, the effects of material non-linearity may be beneficial or detrimental, depending on the circumstances.

RESPONSE TO SIMPLE PULSES

As mentioned earlier, apart from harmonic excitations, simple pulses have also been used in the present study. A simple Ricker pulse with central frequency $f_R = 2\text{Hz}$ has been selected as a pulse excitation [Ricker, 1960]. Despite the simplicity of its waveform, this wavelet covers smoothly a broad range of frequencies up to nearly $3f_R$ ($\approx 6\text{Hz}$). The acceleration time-history and the corresponding Fourier spectrum of this pulse are shown in Figure 8. The height-wise distribution of the normalized induced dynamic earth pressures in the case of the Ricker pulse excitation is plotted in Figure 9, only for three levels of peak base acceleration examined. The pattern revealed in Figure 5 is also present in this case, due to the fact that the used pulse includes a broad range of frequencies close to the fundamental frequency of the retained soil layer ($f_o \approx 3\text{Hz}$), as shown at the Fourier spectrum of the pulse (see Figure 8). As a result, despite the lower levels of earth pressures in this case, the system response is quite similar to that caused by the harmonic excitation at resonance.

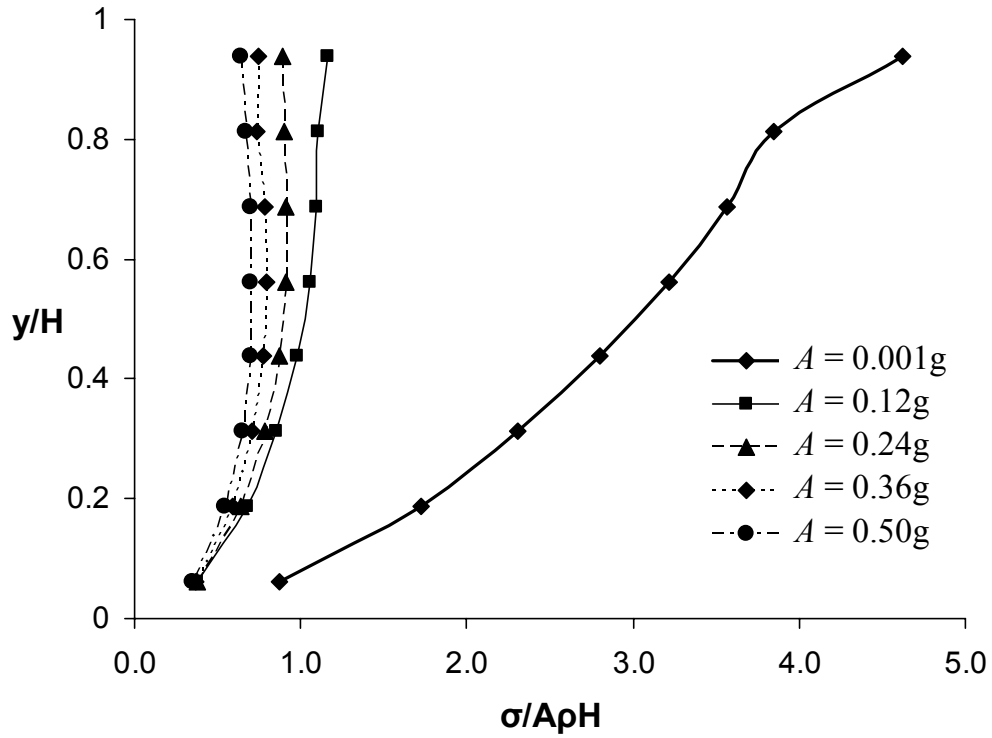


Figure 5. Height-wise distribution of the normalized induced dynamic earth pressures for the harmonic excitation at resonance ($f = f_o$). All five cases of peak base acceleration are shown.

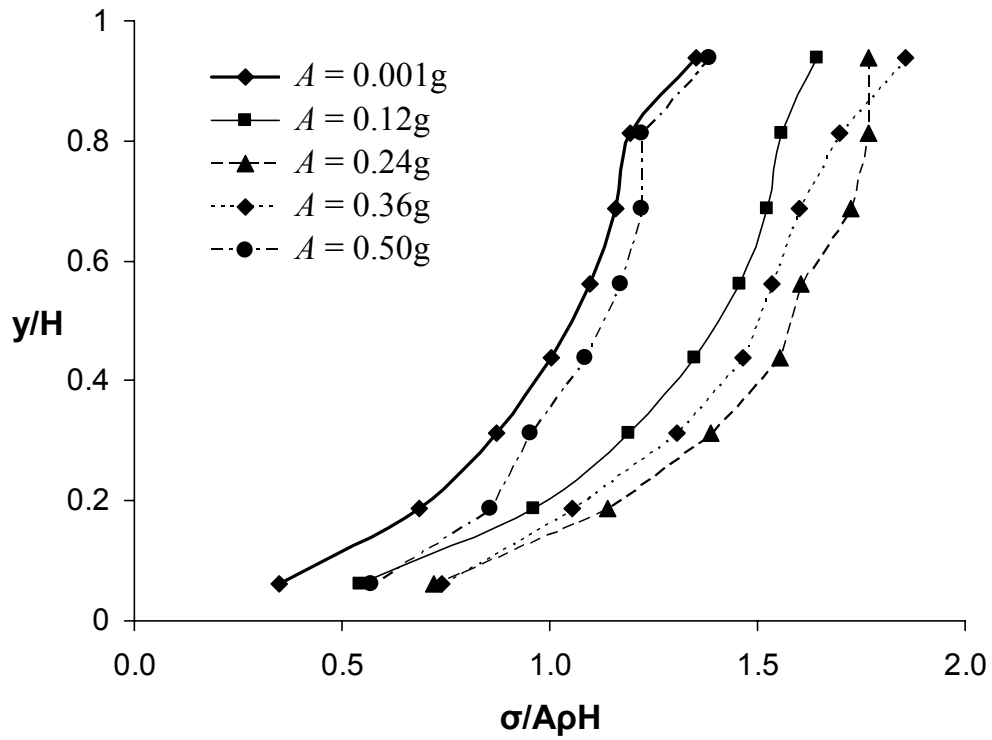


Figure 6. Height-wise distribution of the normalized induced dynamic earth pressures for the low-frequency harmonic excitation ($f = f_o/6$). All five cases of peak base acceleration are shown.

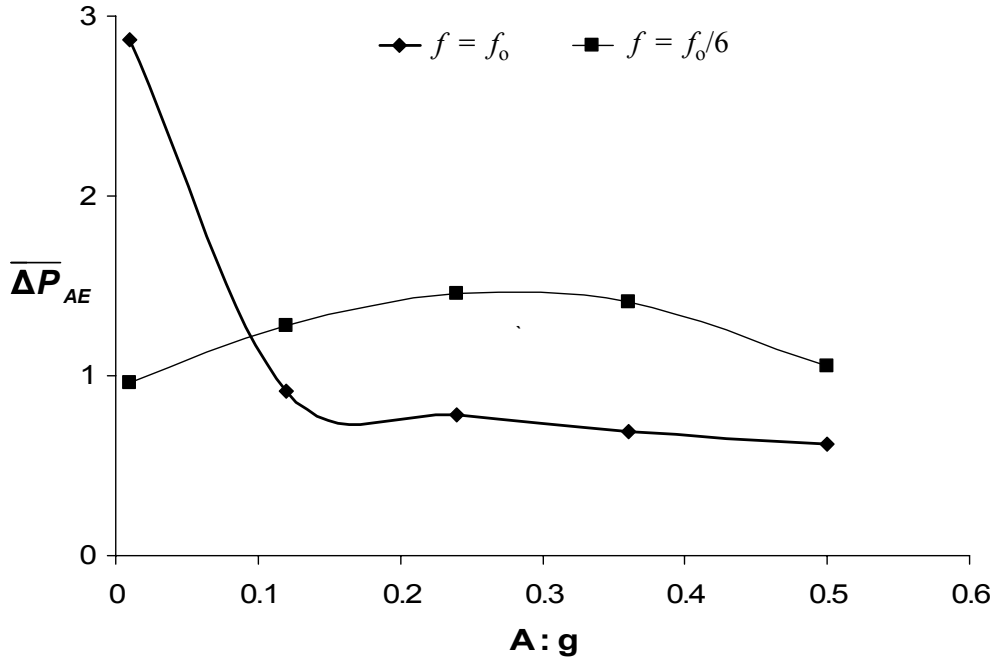


Figure 7. Maximum normalized dynamic earth force as a function of peak base acceleration A , for the two harmonic excitations examined.

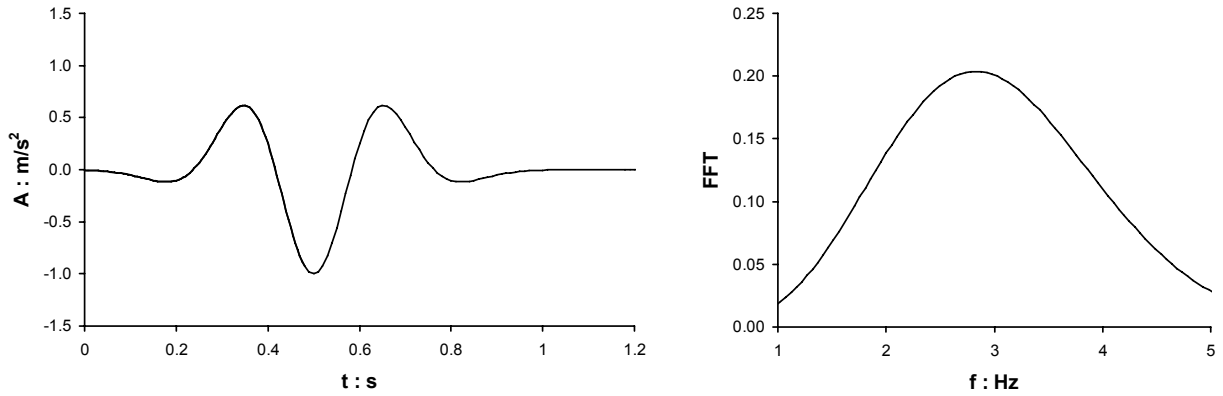


Figure 8. Acceleration time-history (left) (A is scaled to peak acceleration of 1m/s^2) and Fourier spectrum (right) of the Ricker pulse excitation (with central frequency $f_R = 2\text{Hz}$).

As the Ricker pulse covers smoothly the range of frequencies between 1 and 5Hz, it provides an efficient way to comprehend the effect of material non-linearity on the wall distress in the frequency domain as well. Figure 10 shows the variation of the *Pressure Amplification Factor* (PAF) as a function of frequency. PAF is defined as:

$$PAF = \frac{FFT[\overline{\Delta P}_{AE}(t)]}{FFT[A(t)]} \quad (5)$$

where $FFT[\overline{\Delta P}_{AE}(t)]$ is the Fourier spectrum of the normalized induced dynamic earth force time history $\overline{\Delta P}_{AE}(t)$, and $FFT[A(t)]$ is the Fourier spectrum of the acceleration time history of a Ricker pulse excitation with unit peak value (see Figure 8).

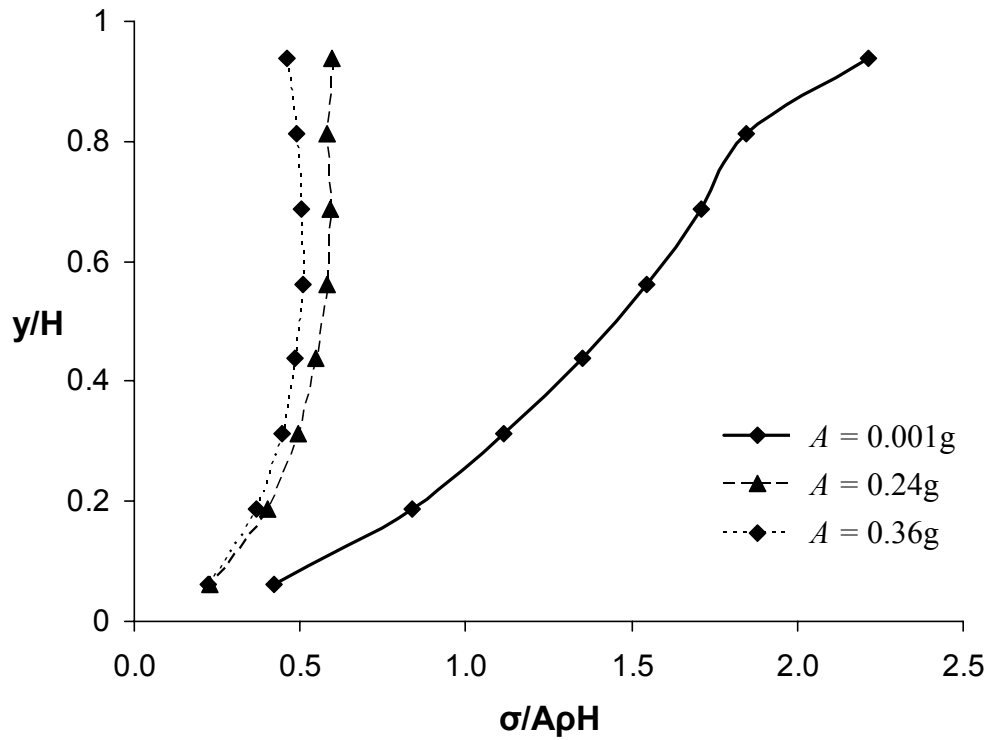


Figure 9. Height-wise distribution of the normalized induced dynamic earth pressures in the case of the Ricker pulse excitation. Three cases of peak base acceleration are examined.

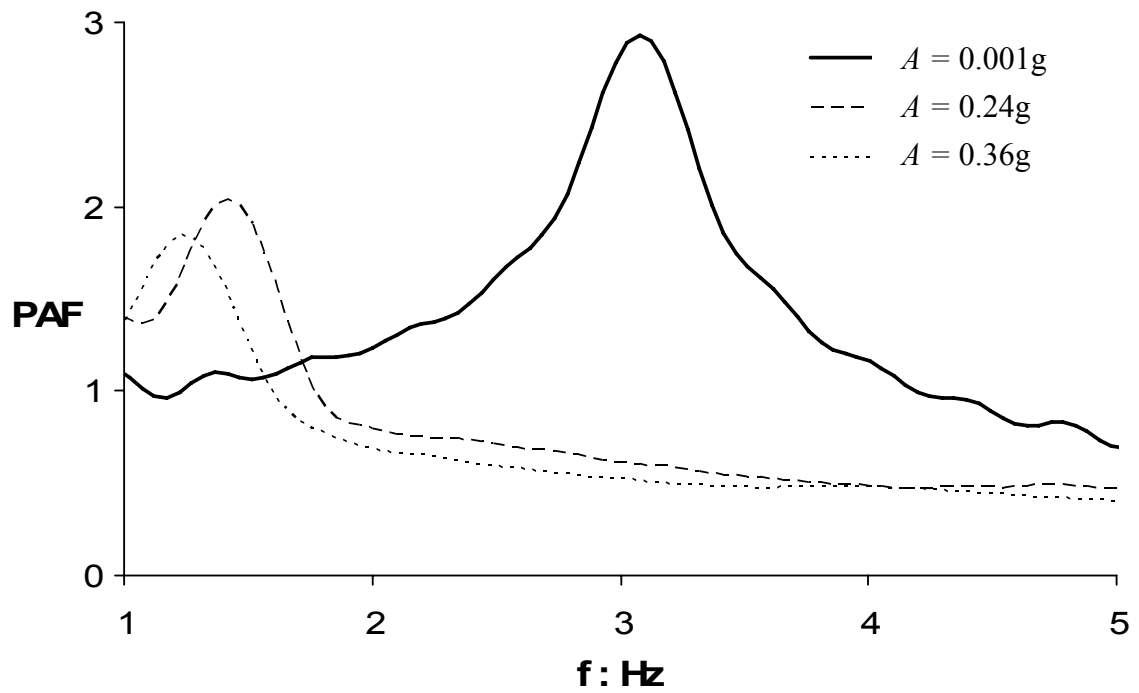


Figure 10. The Pressure Amplification Factors (PAF) calculated for three different levels of peak base acceleration examined.

It is evident that in the case of linear soil behavior the PAF reaches its maximum value for frequencies close to the fundamental frequency of the retained soil layer. This result matches the value calculated in the straightforward way of linear harmonic response at resonance ($\overline{\Delta P_{AE}} \approx 3$). Additionally, for low-frequency excitations, the value of PAF converges to that proposed by Scott (1973) and Wood (1975) and calculated previously. For the case of increased levels of peak base acceleration, the development of material non-linearity not only affects the maximum value of PAF, but also shifts the range of its maximum values towards lower frequencies. This phenomenon can be either beneficial or detrimental, depending on the predominant frequency of the input motion.

Finally, Figure 11 (being actually an extension of Figure 7) shows the maximum normalized dynamic earth force as a function of peak base acceleration A , for the three excitations examined. Note that in the same Figure the values of $\overline{\Delta P_{AE}}$ proposed by Wood (1975) and by Seed & Whitman (1970) are also included as a reference point. It is observed that in the case of linear response, the wall distress is dominated by the frequency content of the excitation. Specifically, $\overline{\Delta P_{AE}}$ varies between the values of 1 and 3, being thus always higher than the standard bounding values adopted by the seismic norms (Wood and M-O). As the degree of non-linearity increases, the distress decreases substantially, ranging between the aforementioned bounds. The only exception seems to be the case of low-frequency (quasi-static) excitation in which $\overline{\Delta P_{AE}}$ reaches a maximum for intermediate levels of peak base acceleration.

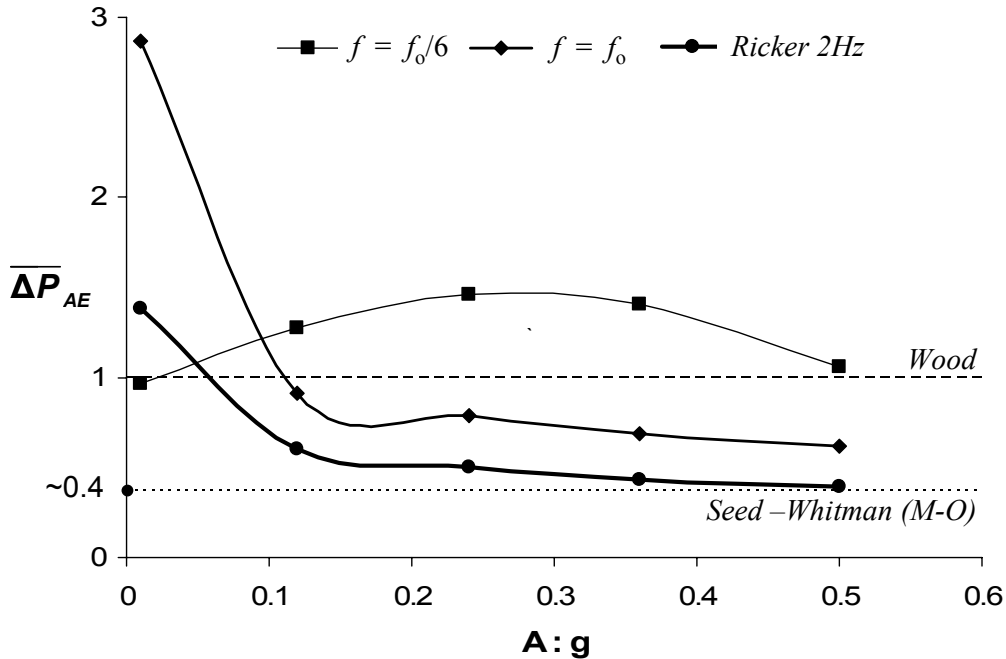


Figure 11. Maximum normalized dynamic earth force as a function of peak base acceleration A , for the three excitations examined. The proposals of Wood (1975) and Seed & Whitman (1970) are also included.

CONCLUSIONS

The present study has examined how and to what extent the potential soil non-linearity, that a retained soil layer may exhibit may affect: (a) the dynamic distress of a rigid non-sliding retaining wall, and (b) the seismic response of the retained soil layer itself. It was found that soil nonlinearity reduces in general the soil amplification of the retained soil and the dynamic earth pressures, leading thus to a lower wall distress. However, as soil nonlinearity alters the eigen-frequencies of the wall-soil system, there exists (under certain circumstances) the possibility that increased nonlinearity may lead to an amplified response. This phenomenon is more probable to occur when the frequency content of the

excitation is narrow and concentrated around a fundamental frequency that is lower than the linear eigen-frequency of the soil layer. In any case, results provide a clear indication that the potential non-linearity increases the degree of complexity, being either beneficial or detrimental for the wall distress, depending on the circumstances. That fact justifies the necessity for a more elaborate consideration of these interrelated phenomena on the seismic design of retaining walls.

ACKNOWLEDGEMENTS

The financial support from the European Union and the General Secretary of Research of Greece (PENED-03/454 research project) is gratefully acknowledged.

REFERENCES

- EAK (2000), Greek Seismic Code, *Greek Ministry of Public Works*, Athens, Greece.
- EC8 (2003), Eurocode 8: Design of structures for earthquake resistance, Part 1, European standard CEN-ENV-1998-1, Draft No. 6, *European Committee for Standardization*, Brussels.
- Green, R.A. and Ebeling, R.M. (2002), Seismic Analysis of Cantilever Retaining Walls, Phase I Report ERDC/ITL TR-02-3, *U.S. Army Corps of Engineers*, Washington, DC.
- Hudson, M.B., Idriss, I.M., and Beikae, M. (1993), QUAD4M : A Computer Program for Evaluating the Seismic Response of Soil-Structures, *Center for Geotechnical Modeling, Department of CEE, Univ. of California*, Davis, California.
- Iai, S. (1998), Seismic analysis and performance of retaining structures, in Dakoulas, P., Yegian M. and Holtz, R.D. (Eds.), *Proc. Geotechnical Earthquake Engineering and Soil Dynamics III*, Geotechnical Special Publ. No. 75, Vol. 2, *ASCE*, Reston, Va., pp. 1020–1044.
- Idriss, I.M. (1990), Response of soft soil sites during earthquakes, in J.M. Duncan (Ed.), *Proceedings, H. Bolton Seed Memorial Symposium*, BiTech Publishers, Vancouver, British Columbia, Vol. 2, pp. 273-289.
- Kramer, S. (1996), *Geotechnical Earthquake Engineering*, *Prentice Hall*.
- Mononobe, N. and Matsuo, H. (1929), On the determination of earth pressures during earthquakes, *Proceedings of the World Engineering Congress*, Tokyo, Japan, Vol. 9, Paper 388.
- Okabe, S. (1926), General theory of earth pressures, *Journal of the Japan Society of Civil Engineering*, 12(1).
- PIANC (2001), International Navigation Association (PIANC): Seismic Design Guidelines for Port Structures, *Balkema Publishers*, Netherlands.
- Psarropoulos, P.N., Klonaris, G. and Gazetas, G. (2005), Seismic earth pressures on rigid and flexible retaining walls, *Soil Dynamics and Earthquake Engineering*, 25, n° 7-10, 795-809.
- Roesset, J.M. (1977), Soil Amplification of Earthquakes, in Desai, C.S. and Christian, J.T. (Eds.), *Numerical Methods in Geotechnical Engineering*, *McGraw-Hill*, pp. 639-682.
- Scott, R.F. (1973), Earthquake-induced pressures on retaining walls, *Proceedings of the 5th World Conference on Earthquake Engineering*, Vol. 2, pp. 1611–1620.
- Seed, H.B. and Idriss, I.M. (1970), Soil moduli and damping factors for dynamic response analyses, *Report EERC 70-10*, Earthquake Engineering Research Center, University of California, Berkeley.
- Seed, H.B. and Whitman, R.V. (1970), Design of earth retaining structures for dynamic loads, *Proceedings of the Special Conference on Lateral Stresses in the Ground and Design of Earth Retaining Structures*, *ASCE*, pp. 103–147.
- Veletsos, A.S. and Younan, A.H. (1997), Dynamic Response of Cantilever Retaining Walls, *ASCE Journal of Geotechnical and Geoenvironmental Engineering*, 123 n° 2, 161–172.
- Wood, J.H. (1975), Earthquake – Induced Pressures on a Rigid Wall Structure, *Bulletin of New Zealand National Earthquake Engineering*, 8, 175–186.
- Wu, G. and Finn, W.D.L. (1999), Seismic lateral pressures for design of rigid walls, *Canadian Geotechnical Journal*, 36, n° 3, 509-522.